

**BIOSYNTHESIS OF ENDOSOME-SPECIFIC
LIPID BIS(MONOACYLGLYCERO)PHOSPHATE**

LIM SHI ROU

UNIVERSITI SAINS MALAYSIA

2018

**BIOSYNTHESIS OF ENDOSOME-SPECIFIC
LIPID BIS(MONOACYLGLYCERO)PHOSPHATE**

by

LIM SHI ROU

**Thesis submitted in fulfillment of the requirements
for the Degree of
Doctor of Philosophy**

March 2018

ACKNOWLEDGEMENT

First and foremost, I would like to express my sincerest appreciation to Professor Dr. Gam Lay Harn, Dr. Peter Greimel, Dr. Hullin-Matsuda Francoise, Dr. Toshihide Kobayashi, and Professor Dr. Kumar Sudesh, for giving me the golden opportunity to pursue Doctor of Philosophy degree program at Lipid Biology Laboratory, RIKEN, Japan under the agreement for International Joint Graduate School Program between RIKEN and Universiti Sains Malaysia (USM).

Most importantly, my deepest appreciation expressed to Dr. Peter Greimel and Dr. Hullin-Matsuda Francoise for their boundless guidance, inspiration and valued experience sharing which impacted on my life. Special thanks delivered to Dr. Hullin-Matsuda Francoise and her research team from INSERM, France, for the collaboration of sub-project described in the present dissertation.

I would like to deliver thousands of appreciation to Ministry of Higher Education Malaysia for the offer of MyPhD Sponsorship Program, and RIKEN for the offer of living allowance, which were the financial support throughout my studies.

I would like to extend my gratitude to the secretaries from Lipid Biology Laboratory RIKEN, Ogura-san, Saito-san and Toyoda-san. Also, the support provided by Global Relations Office, RIKEN should be appreciated, especially Maya Kobayashi-san.

I am thankful to my labmates, Dr. Neval Yilmaz, Dr. Hui Hui Tan, Dr. Sabrina Kargoll and Dr. Yan Fen Lee, who often shared their useful suggestion or comment on my work, and also their encouragement and concern.

Last but not least, thank you very much to my beloved family for their concern, love and spiritually support.

TABLE OF CONTENTS

Acknowledgement	ii
Table of Contents	iii
List of Tables	ix
List of Figures	xii
List of Abbreviations	xxi
List of Appendices	xxvi
Abstrak	xxvii
Abstract	xxix
CHAPTER 1 LITERATURE REVIEW	1
1.1 Lipid overview	1
1.2 Membrane phospholipids	10
1.3 Biosynthesis of phospholipids	12
1.4 Bis(monoacylglycero)phosphate (BMP)	15
1.4.1 Structure and <i>de novo</i> biosynthesis of BMP	15
1.4.2 Cellular localization and biological roles of BMP	19
1.4.3 Proposed biosynthetic pathway of BMP from PG	21
1.4.3(a) Phospholipase and transacylase	21
1.5 Research background of BMP	26
1.6 Current research topic of BMP and general objectives	30
1.7 Headlines of general objectives	31
CHAPTER 2 GENERAL METHODOLOGY	32
2.1 Cell culture and harvest	32
2.2 Preparation of lipid stock and internal standard	34

2.3	Lipid extraction	34
2.3.1	Modified Bligh and Dyer procedure	34
2.4	Preparation of liposomes	36
2.4.1	Multilamellar vesicles	36
2.4.2	Small unilamellar vesicles	36
2.5	Determination of protein concentration	38
2.5.1	Bradford protein assay	38
2.5.2	Pierce BCA protein assay	39
2.6	Liquid chromatography coupled with mass spectrometric analysis of phospholipids	39

CHAPTER 3 CONVERSION OF PG TO BMP IN RAW 264.7 MACROPHAGES 42

3.1	Introduction and Objectives	42
3.2	Materials and Methods	51
3.2.1	Acyl species specificity of the PG-BMP enzymatic conversion	51
3.2.2	Time course of cellular uptake of OO PG and BMP/AcPG biosynthesis	51
3.2.3	Pulse chase experiment	52
3.2.4	Time course of BMP and AcPG biosynthesis	52
3.2.5	Analysis of neutral and acidic lipids in culture medium and cells	53
3.2.6	Time course of cell neutral lipid biosynthesis	54
3.2.7	Elucidation of native regioisomer of BMP in mammalian cells	55
3.3	Results and Discussion	56
3.3.1	RAW 264.7 cells treatment with exogenous PG	56
3.3.1(a)	PG acyl species substrate specificity for BMP biosynthesis	56
3.3.1(b)	Uptake of OO PG by RAW 264.7 cells	66
3.3.1(c)	Pulse chase experiment with OO PG	71

3.3.1(d)	Time course of biosynthesis of BMP and AcPG in cells during incubation with exogenous OO PG	75
3.3.1(e)	Presence of neutral lipids and phospholipids in and outside the cells	81
3.3.1(f)	Time course of biosynthesis of neutral lipids in the cells	89
3.3.2	RAW 264.7 cells treatment with dioleoyl BMP	99
3.3.2(a)	Elucidation of native regioisomer of BMP in mammalian cells	99
CHAPTER 4 EFFECT OF AMIODARONE ON BMP AND AcPG IN RAT LIVER		110
4.1	Introduction and Objectives	110
4.2	Materials and Methods	112
4.2.1	Administration of drug to rat	112
4.2.2	Sampling of rat liver	113
4.2.3	Lipid extraction and analysis	114
4.3	Results and Discussion	115
CHAPTER 5 <i>IN VITRO</i> BIOSYNTHESIS OF BMP AND AcPG		123
5.1	Introduction and Objectives	123
5.2	Materials and Methods	127
5.2.1	Screening for PLA and TA activity	127
5.2.2	Kinetic of AcPG formation	128
5.2.3	Substrate of PLA and TA	129
5.2.4	Effect of substrate concentration on PLA and TA activity	130
5.2.5	Effect of heat on PLA and TA activity	131
5.2.6	Effect of divalent cations on PLA and TA activity	132
5.2.7	Effect of PLA inhibitors on PLA and TA activity	134

5.2.8	Potential acyl donor for TA	136
5.2.9	PLA and TA activity in serum of fetal bovine, goat, horse and human	138
5.2.10	Established assay condition for PLA and TA activity	140
5.3	Results and Discussion	142
5.3.1	Screening for PLA and TA activity	142
5.3.2	Method development of <i>in vitro</i> assay for biosynthesis of AcPG	146
5.3.2(a)	Kinetic of AcPG formation	147
5.3.2(b)	Substrate specificity of phospholipase-transacylase activity	150
	5.3.2(b)(i) PG	150
	5.3.2(b)(ii) BMP	153
5.3.2(c)	Effect of substrate concentration on AcPG synthesis rate	156
5.3.2(d)	Effect of heat on AcPG biosynthetic activity in FBS	159
5.3.2(e)	Effect of divalent cations on AcPG biosynthetic activity in FBS	161
5.3.2(f)	Effect of PLA inhibitors on AcPG biosynthetic activity in FBS	166
5.3.3	Potential acyl donor for AcPG biosynthetic activity in FBS	169
5.3.4	AcPG biosynthetic activity in serum of fetal bovine, goat, horse and human	172
5.3.5	Evaluation of assay establishment for the biosynthesis of AcPG	175
5.3.6	Comparison of AcPG biosynthetic activity between <i>in vivo</i> and <i>in vitro</i> experiment	177

CHAPTER 6 ENRICHMENT, IDENTIFICATION AND CHARACTERIZATION OF AcPG ASSOCIATED ACYLTRANSFERASE	180
6.1 Introduction and Objectives	180
6.2 Materials and Methods	188
6.2.1 Protein enrichment from FBS	188
6.2.2 Sodium dodecyl sulphate-polyacrylamide gel electrophoresis	191
6.2.3 Identification of proteins purified from FBS	192
6.2.4 Protein-liposomes binding assay	193
6.2.5 Effect of serum filtration and roles of lipoprotein on enzymatic activity	194
6.2.6 Separation of lipoprotein from FBS by density gradient ultracentrifugation	195
6.2.7 Cellular localization of protein	198
6.2.7(a) Time course of protein secretion from RAW 264.7 macrophages	199
6.2.7(b) Peak time of protein secretion from RAW 264.7 macrophages	199
6.2.8 Identification of proteins secreted from RAW 264.7 macrophages	200
6.3 Results and Discussion	201
6.3.1 Method development for protein enrichment from FBS	201
6.3.1(a) Ammonium sulfate precipitation and dialysis	202
6.3.1(b) Size exclusion and weak anionic chromatography	205
6.3.1(c) Size exclusion and strong anionic chromatography	210
6.3.1(d) Hydrophobic interaction and strong anionic chromatography	213
6.3.1(e) Reproducibility of protein purification method	218

6.3.2	Identification of enriched proteins from FBS	221
6.3.3	Alternative identification and enrichment strategies	227
6.3.3(a)	Protein-liposomes binding assay	227
6.3.3(b)	Effect of serum filtration and role of lipoprotein on enzymatic activity	230
6.3.3(c)	Lipoprotein density gradient ultracentrifugation using potassium bromide	236
6.3.4	Cellular localization of AcPG forming activity	240
6.3.4(a)	Time course of protein secretion from RAW 264.7 macrophages	243
6.3.4(b)	AcPG and BMP forming activities secreted from RAW 264.7 macrophages	246
6.3.5	Identification of protein secreted from RAW 264.7 macrophages	249
	CHAPTER 7 GENERAL REVIEW	252
	CHAPTER 8 CONCLUSION	256
	CHAPTER 9 CONTRIBUTION AND FUTURE PERSPECTIVE	260
	REFERENCES	263
	APPENDICES	

LIST OF TABLES

		Page
Table 1.1	Physiologically relevant fatty acids (Fahy <i>et al.</i> , 2005)	8
Table 1.2	Selected publications related to BMP from year 1967-2012	27
Table 3.1	PG consisting of three combinations of acyl chains were supplied to RAW 264.7 cells. For simplicity, the indicated abbreviations will be used throughout this document	44
Table 3.2	Fatty acid composition (%) of BMP and AcPG isolated from BHK cells (Brotherus and Renkonen, 1974)	44
Table 3.3	Utilized commercial BMP with its respective glycerophosphoglycerol backbone stereoconfiguration (Avanti® Polar Lipids, Inc.) for RAW 264.7 cells treatment	46
Table 3.4	Conversion of <i>sn</i> -3,3' BMP to <i>sn</i> -3,2' BMP and <i>sn</i> -2,2' BMP upon 24 hours of RAW 264.7 macrophages treatment with R,R' BMP, R,S' BMP and S,S' BMP. Blue line, original LC-MS data; red dotted line, fitted data for a single regioisomer based on Gaussian distribution; green line, sum of fitted data	102
Table 5.1	Commonly used buffer systems for <i>in vitro</i> biochemical assay (Labome, The world of laboratories)	125
Table 5.2	Assay condition used for screening of PLA and TA activity	128
Table 5.3	Assay condition for PLA and TA activity. Parameter tested: Incubation time	129
Table 5.4	Assay condition for PLA and TA activity. Parameter tested: Types of substrate	130

Table 5.5	Assay condition for PLA and TA activity. Parameter tested: Concentration of substrate	131
Table 5.6	Assay condition for PLA and TA activity. Parameter tested: Effect of heat	132
Table 5.7	Assay condition for PLA and TA activity. Parameter tested: Effect of divalent cations	134
Table 5.8	Assay condition for PLA and TA activity. Parameter tested: Effect of PLA inhibitors	136
Table 5.9	Assay condition for PLA and TA activity. Parameter tested: Potential acyl donor for TA	138
Table 5.10	Assay condition for PLA and TA activity. Parameter tested: Different sources of serum	139
Table 5.11	Annotation for the legends shown in figure 5.10	161
Table 5.12	Optimized parameter for <i>in vitro</i> formation of AcPG from PG	175
Table 5.13	<i>In vivo</i> and <i>in vitro</i> conversion of PG to AcPG and LPG	178
Table 6.1	Physical property of biomolecules and column chromatography technique (Coskun, 2016)	183
Table 6.2	Protocol for gel silver staining	192
Table 6.3	Lipid compositions of liposomes employed for binding assay	193
Table 6.4	Description for each of the gel lane shown in figure 6.5	208
Table 6.5	Annotation for each of the fraction shown in figure 6.8	216
Table 6.6	Partial purification of TA activity from FBS. <i>n</i> denotes the experiment number	219

Table 6.7	List of candidate proteins involved in the biosynthesis of AcPG from PG	223
Table 6.8	Similarity of vanin-1 or pantetheinase of <i>Bos taurus</i> with organisms of Archaea, Bacteria and Human domain	227
Table 6.9	Employed lipid composition of each gel lane shown in figure 6.12	229
Table 6.10	Annotation for each gel lane shown in figure 6.15	239
Table 6.11	Assays incubated with upper fraction, middle fraction and lowest fraction collected from density gradient ultracentrifugation and non-heated FBS as control	240
Table 6.12	Annotation for each of gel lane as shown in figure 6.21	250

LIST OF FIGURES

	Page
Figure 1.1: Representative structure for each of the lipid classes (Fahy <i>et al.</i> , 2005)	3
Figure 1.2: Assignment of S and R enantiomers following CIP rules. In this example the priority groups are read a > b > c > d (Willock, 2009)	6
Figure 1.3: Structure of a fatty acid chain which consists of a carboxyl head group and a hydrocarbon tail (Fahy <i>et al.</i> , 2005)	8
Figure 1.4: Schematic illustration of liposomes of different sizes, including small unilamellar vesicle (SUV), large unilamellar vesicle (LUV), multilamellar vesicle (MLV) and multivesicular vesicle (MVV) (http://www.azonano.com/article.aspx?ArticleID=1243)	10
Figure 1.5: Representative structures of common phospholipids (Kelly and Jacobs, 2016)	12
Figure 1.6: Comparison of the biosynthetic pathways of phospholipids in archaea, bacteria and eukaryotes (Lombard <i>et al.</i> , 2012)	14
Figure 1.7: Stereoconfiguration of BMP: <i>sn</i> -1,1' diglycerophosphate	17
Figure 1.8: The <i>de novo</i> biosynthesis of BMP from PA. The enzymes catalysing the successive steps from PG to BMP have not been characterized yet. Red squares indicate the altered backbone configuration between PG and BMP	18
Figure 1.9: Endocytosis via early endosome, late endosome and lysosome (Scott <i>et al.</i> , 2014)	20
Figure 1.10: Ester bond specificity of phospholipases (Richmond and Smith, 2011)	23

Figure 1.11:	Proposed biosynthetic pathway of BMP from PG. PLA ₂ : Phospholipase A2; TA: Transacylase; PL: Phospholipid; LPL: Lysophospholipids; ROE: Reorientation of enzyme (Amidon <i>et al.</i> , 1995)	24
Figure 1.12:	Alternative routes for biosynthesis of BMP from PG (Poorthuis and Hostetler, 1976)	25
Figure 2.1:	Parts of Avanti mini extruder (A) with the heating block (B) (cited from http://avantilipids.com/divisions/equipment/)	37
Figure 3.1:	Structure of PG purchased from Avanti® Polar Lipids, Inc. Example shown is OO PG (sometimes referred as 18:1,18:1 PG) formulated as sodium salt (Na ⁺). C2 and C2' indicate the chiral atoms featuring R and S stereoconfiguration, respectively	43
Figure 3.2:	Structure of OO (R,S')-BMP ammonium salt (NH ₄ ⁺) purchased from Avanti® Polar Lipids, Inc. C2 and C2' indicate the chiral carbon atoms of the respective glycerol. Red numbers correspond to the stereospecific numbering convention	46
Figure 3.3:	Spontaneous acyl migration depicted in S,S'-BMP can lead to up to three different, but interconvertible regioisomers	47
Figure 3.4:	Comparison of LPG dependent and AcPG dependent conversion of PG to BMP. FA: Fatty acid; PLA ₂ : Phospholipase A2; PLA ₁ : Phospholipase A1; Lyso-PL: Lysophospholipid; PL: Phospholipid	49
Figure 3.5:	Total BMP content of RAW 264.7 cells upon 24 hours of incubation with 50 μM of PG featuring different acyl chains	57
Figure 3.6:	AcPG content of RAW 264.7 cells after 24 hours of incubation with different species of 50 μM of PG	62
Figure 3.7:	Zoomed multiple reaction monitoring (MRM) chromatogram of 18:1,18:1-18:1AcPG	63

Figure 3.8:	Presence of phospholipids within the cells and in the medium of RAW 264.7 cells cultured for the indicated time in the presence of OO PG	67
Figure 3.9:	AcPG content in the cell culture medium and inside of RAW 264.7 cells cultured for the indicated time in the presence of OO PG	68
Figure 3.10:	LPG content inside and in the cell culture medium of RAW 264.7 cells cultured for the indicated time in the presence of OO PG (zooming from Fig. 3.7)	69
Figure 3.11:	BMP content in the cell culture medium of RAW 264.7 cells cultured for the indicated time in the presence of OO PG compared to control cells	70
Figure 3.12:	PG (A), BMP (B), AcPG (C) and LPG (D) content in the cells upon removal of PG at the indicated time followed by incubation up to 24 hours prior to analysis	73
Figure 3.13:	Time course of the conversion of 50 μ M OO PG to BMP, AcPG and LPG in RAW 264.7 cells at time points of 0, 1, 2, 3, 6, 8 and 24 hours. PG and BMP (A), LPG (B) and AcPG (C) contents in cells	76
Figure 3.14:	Proposed biosynthetic pathway of BMP from PG via AcPG, as outlined in route 1. Route 2 shows the classical biosynthetic pathway of BMP from PG via LPG	79
Figure 3.15:	Neutral lipids in RAW 264.7 macrophages upon 8 hours of incubation with 18:1,18:1 PG (OO PG) and 18:0,18:1 PG (SO PG) (A). Standard of neutral lipids (B). The legends for spots of TLC are shown as above:	83
Figure 3.16:	Acidic phospholipids in cell medium of RAW 264.7 macrophages upon 8 hours incubation with OO PG and SO PG (A). Standard of acidic phospholipids (B). The legends for spots of TLC are shown as above:	86

Figure 3.17:	Comparison between lipid standard and individual acidic lipid species	88
Figure 3.18:	Biosynthesis of neutral lipids in RAW 264.7 macrophages at time points of 0, 4, 8 and 24 hours (A). Neutral lipid standard (B)	91
Figure 3.19:	Biosynthesis of TAG in RAW 264.7 macrophages upon OO PG treatment at time points of 0, 1, 2, 4, 8, and 24 hours, based on TLC visualization. Standard deviation is of triplicate reading	92
Figure 3.20:	Proposed biosynthesis of S,S' BMP and R,S' AcPG from exogenous PG via PLC and lipases activity. DAG: Diacylglycerol; G1P: Glycerol-1-Phosphate; FFA: Free fatty acid; MAG: Monoacylglycerol; DGAT: Diacylglycerol acyltransferase; FA-CoA: Fatty acid coenzyme A ester; PA: Phosphatidic acid; PGPS: Phosphatidylglycerol phosphate synthase(*) denotes fatty acid pools released from various PG molecules can be either used for formation of BMP or AcPG	96
Figure 3.21:	Spontaneous ester migration demonstrating interconversion of the three possible regioisomers of BMP	100
Figure 3.22:	Individual content of each of the three possible regioisomers of BMP in RAW 264.7 cells at different time points upon treatments of R,R' BMP (B), R,S' BMP (C) and S,S' BMP (D) and control (A)	106
Figure 4.1:	Structure of Amiodarone (Cordarone®)	110
Figure 4.2:	Effect of 8 days oral treatment of amiodarone on the content of BMP (A), AcPG (B) and PG (C) in rat liver. Amio50 and amio150 represent the amiodarone administration of 50 mg/kg and 150 mg/kg to rat, respectively. Only the major lipid species are reported	119
Figure 5.1:	Flow chart outlining assay optimization for PLA and TA activity involved in the biosynthesis of AcPG and/ or BMP	141

Figure 5.2:	Formation of BMP (A) and AcPG (B) from dioleoyl PG in a total reaction volume of 3 mL. SUVs denote small unilamellar vesicles and MLVs denote multilamellar vesicles. Specific activity of enzymes is expressed as nmol/mg of protein. Data is of duplicate reading	144
Figure 5.3:	Simplified diagram of SUV (A) and MLV (B)	145
Figure 5.4:	Formation of AcPG (A) and LPG (B) as a function of time. Ctl 1 (control 1) consists of 10 % non-heated FBS without addition of OO PG; ctl 2 (control 2) consists of OO PG without addition of non-heated FBS; exp (experiment) consists of both 10 % non-heated FBS and OO PG	149
Figure 5.5:	Enzymatic assay of conversion of PG (A) to AcPG (B) and LPG (C) in a total volume of 2 mL. Standard deviation is of triplicate reading	152
Figure 5.6:	Influence of BMP stereoconfiguration on the formation of AcPG (A) and LPG (B)	154
Figure 5.7:	Lineweaver-Burk linearization of experimental data to estimate K_M and V_{max}	157
Figure 5.8:	Interpretation of biosynthesis of AcPG based on Michaelis-Menten principle	158
Figure 5.9:	Effect of heat treatment of FBS on formation of AcPG (A) and LPG (B). Palmitoyl LPG denotes 1-palmitoyl-2-hydroxy lyso phosphatidylglycerol; Oleoyl LPG denotes 1-hydroxy-2-oleoyl lyso phosphatidylglycerol; NH FBS denotes non-heated fetal bovine serum; H FBS denotes heated fetal bovine serum. Standard deviation is of triplicate reading	160
Figure 5.10:	Effect of divalent cations on AcPG biosynthetic activity in FBS. AcPG (A), palmitoyl LPG (B) and oleoyl LPG (C). AcPG measured in the assay is referred to PO-P species	163

Figure 5.11:	Effect of PLA inhibitors on AcPG (A) and LPG (B) formation. Small letter of t denotes incubation time. Standard deviation is of triplicate reading	167
Figure 5.12:	Potential acyl donor for TA. Mixture of total 30 μ M of 16:0,18:1 PG (PO PG) with each of the following lipids, C16 FA: carbon-16 fatty acid (palmitic acid); TAG: trioleoylglycerol; PC: 16:0-18:1 PC (PO PC); PC+FBS lipid: PC (PO PC) added with lipid from FBS. P CE: palmitoyl cholesteryl ester; O CE: oleoyl cholesteryl ester. Only PO-P species of AcPG was measured as enzymatic product	170
Figure 5.13:	Formation of AcPG (A), palmitoyl LPG (B), oleoyl LPG (C) from PG (D) by using serum of fetal bovine, goat, horse and human	174
Figure 6.1:	Basic components of a typical MS (modified from Dass, 2001)	186
Figure 6.2:	Flow chart outlining protein enrichment from FBS	191
Figure 6.3:	Fractionation of lipoprotein from FBS by using density gradient ultracentrifugation	197
Figure 6.4:	Gradient (4-15 %) SDS-PAGE profiles of ammonium sulfate precipitated-proteins from FBS. Lane 1: 100-fold diluted FBS; Lane 2 and 6: Molecular weight protein marker; Lane 3: 0-15 % salt-saturated (F1); Lane 4: 15-25 % salt-saturated (F2); Lane 5: 25-35 % salt-saturated (F3)	203
Figure 6.5:	Gradient (4-15 %) SDS-PAGE profiles of three successive steps of protein fractionation. Gel was stained with Coomassie blue R-250. The annotation for each of the lane is shown in table 6.3 as below:	207
Figure 6.6:	Enzymatic formation of AcPG using DEAE A25 chromatography-eluted fractions (100-1000 mM NaCl) after 0-25 % ammonium sulfate protein precipitation and Sephadex G50 chromatography purification. Assay was incubated in a total volume of 2 mL	209

Figure 6.7:	Elution profiles of protein fractionated through Sephadex 50 chromatography and Q Sepharose chromatography. Protein was enriched prior to Sephadex 50 chromatography. Gel was stained with Coomassie blue R-250	212
Figure 6.8:	Enzymatic assay for AcPG formation using protein fractions collected from Q Sepharose chromatography elution. PO PG was supplied as substrate and PO-P AcPG was measured as enzymatic product. Annotation for each fraction is summarized in table 6.5 (below)	216
Figure 6.9:	Enzymatic formation of AcPG in 4 hours-assay incubated with the partially purified protein from FBS. P and O denote palmitic acid and oleic acid, respectively	217
Figure 6.10:	Gradient SDS-PAGE (4-15 %) protein profile of three successive steps of purification. Lane 1: Molecular weight protein marker; Lane 2: 100-fold diluted FBS; Lane 3: 10-fold diluted protein precipitated after ammonium salt precipitation; Lane 4: after Octyl Sepharose column; Lane 5: after Q Sepharose column. The proteins were visualized with silver stain. 1 μ g of protein was loaded into each well	221
Figure 6.11:	Involvement of Vanin in hydrolysis of pantetheine to pantothenate and cysteamine (Kaskow <i>et al.</i> , 2012)	225
Figure 6.12:	Gradient (4-15 %) SDS-PAGE protein profile of protein-liposome binding fraction. The gel was visualized with Coomassie blue R-250. The annotation for each lane is summarized in table 6.9	229
Figure 6.13:	Formation of AcPG (A), palmitoyl lyso PG (B) and oleoyl lyso PG (C) from 16:0,18:1 PG (PO PG). Final content of enzymatic products is expressed as concentration (μ M). Data is of triplicate reading	233

- Figure 6.14: Formation of AcPG (A), palmitoyl lyso PG (B) and oleoyl lyso PG (C) from 16:0,18:1 PG (PO PG). Content of enzymatic products is expressed as specific activity (nmol/mg protein). Data is of triplicate reading 234
- Figure 6.15: Gradient SDS-PAGE (4-15 %) protein fractions collected from lipoprotein density gradient ultracentrifugation. (A): Coomassie Blue Staining; (B): silver staining. A total of 1 µg of protein was loaded into each well. Upper fractions were loaded in 10-fold dilution. Middle and lowest fractions, non-heated lipoprotein deficient serum and non-heated fetal bovine serum were loaded in 100-fold dilution. Annotation for each gel lane is shown in table 6.10 238
- Figure 6.16: Formation of PO-P AcPG, P LPG and O LPG in assay incubated with cell supernatant upon 4 hours of incubation. Pure MEM and MEM added with 10 % of FBS were collected as cell supernatant. P and O denote palmitoyl and oleoyl, respectively. Data is of triplicate reading 242
- Figure 6.17: Formation of AcPG (A) and LPG (B) in assay incubated with cell supernatant consisting of pure MEM which was collected upon 1, 2, 4, 8 and 12 hours of incubation. Small letter of 't' defines the assay incubation time in hours. Data is of triplicate reading 244
- Figure 6.18: Gradient (4-15 %) SDS-PAGE protein profile of protein secretion from RAW 264.7 cells at time points of 0, 1, 2, 4, 8 and 12 hours, as displayed in lane 2, 3, 4, 5, 6 and 7 accordingly. Lane 1 shows molecular weight protein marker. Gel was visualised with silver staining. 2 µg of protein were loaded into each well 246
- Figure 6.19: Formation of AcPG, LPG and BMP in *in vitro* assay incubated with concentrated cell supernatant after 2 hours incubation with pure MEM. P and O denote palmitoyl and oleoyl species, respectively.

	Ctl denotes control, exp denotes experiment. The <i>in vitro</i> assay was incubated for 4 hours. Data is of triplicate reading	248
Figure 6.20:	Formation of BMP from PG via transacylase activity	249
Figure 6.21:	Gradient (4-20 %) SDS-PAGE protein profile of cell supernatant and cell lysate collected upon 4 hours of incubation with MEM or MEM containing 10 % FBS. The gel was visualized with silver staining and lane annotation is summarized in table 6.12	250

LIST OF ABBREVIATIONS

1,2- <i>sn</i> -DAG	1,2- <i>sn</i> -diacylglycerol
2,3- <i>sn</i> -DAG	2,3- <i>sn</i> -diacylglycerol
AACOCF ₃	Arachidonyl trifluoromethyl ketone
AC	Affinity chromatography
AcPG	Acyl phosphatidylglycerol
ALA	α -Linolenic acid/ Linolenate
ATGL	Adipose triglyceride lipase
ATP	Adenosine triphosphate
BEL	Bromo-enol lactone
BHK	Baby hamster kidney
BHT	Butylated hydroxytoluene
BMP	Bis(monoacylglycerol)phosphate
BPA	Bisphosphatidic acid
BSA	Bovine serum albumin
B&D	Bligh and Dyer
CAD	Cationic amphiphilic drug
CAD	Collision activated dissociation
CDP-DAG	Cytidine diphosphate-diacylglycerol
CE	Cholesteryl ester
CE	Collision energy
CF	Chromatofocusing
CHO	Chinese Hamster Ovary

CIP	Cahn-Ingold-Prelog
CL	Cardiolipin
cPLA2	Cytosolic phospholipase A2
CUR	Curtain gas flow
CXP	Collision cell exit potential
DAG	Diacylglycerol
DEAE A25	Diethylaminoethyl A25
DHA	Docosaehaenoic acid
diDHA	Didocosaehaenoic acid
DMBMP	Bis(monoacylglycero)phosphate (S, R isomer)
DMPG	1,2-dimyristoyl- <i>sn</i> -glycero-3-phospho-(1'-rac-glycerol)
DMSO	Dimethyl sulfoxide
DP	Declustering potential
EDTA	Ethylenediaminetetraacetic acid
EE	Early endosome
EP	Entrance potential
EPA	Eicosapentaenoic acid
ER	Endoplasmic reticulum
ESI	Electrospray ionization
EVs	Extracellular vesicles
FBS	Fetal bovine serum
G1P	Glycerol-1-phosphate
G3P	Glycerol-3-phosphate
GF	Gel filtration
HDL	High density lipoprotein
HED	Human equivalent dose
HEPES	4-(2-Hydroxyethyl)-1-piperazineethanesulfonic acid
HIC	Hydrophobic interaction chromatography
HILIC	Hydrophilic interaction liquid

HPLC	chromatography High performance liquid chromatography
HPTLC	High performance thin layer chromatography
IEC	Ion exchange chromatography
Ihe	Interface heater
IS	Ion spray
IUBMB	International Union of Biochemistry and Molecular Biology
IUPAC	International Union of Pure and Applied Chemistry
IV	Intravenous
LBPA	Lysobisphosphatidic acid
LC-MS	Liquid chromatography coupled with mass spectrometry
LC-MS/MS	Liquid chromatography coupled with tandem mass spectrometry
LDL	Low density lipoprotein
LE	Late endosome
LPA	Lysophosphatidic acid
LPG	Lysophosphatidylglycerol
LPL	Lysophospholipid
LSDs	Lysosomal storage disorders
LUV	Large unilamellar vesicles
LysoPLA1/2	Lysophospholipase A1/2
MAFP	Methyl arachidonyl fluorophosphate
MAG	Monoacylglycerol
MEM	Minimal essential medium
MLVs	Multilamellar vesicles
MOPS	3-(<i>N</i> -morpholino)propanesulfonic acid
MRM	Multiple reaction monitoring
MVVs	Multivesicular vesicles

NMR	Nuclear magnetic resonance
OOO TAG	Trioleoylglycerol
O CE	Oleoyl cholesteryl ester
PA	Phosphatidic acid
PBS	Phosphate buffer saline
PC	Phosphatidylcholine
P CE	Palmitoyl cholesteryl ester
PE	Phosphatidylethanolamine
PG	Phosphatidylglycerol
PGP	Phosphatidylglycerophosphate
PI	Phosphatidylinositol
pI	Isoelectric point
PL	Phospholipid
PLA	Phospholipase
PLA1	Phospholipase A1
PLB	Phospholipase B
PLC	Phospholipase C
PLD	Phospholipase D
PNS	Post nuclear supernatant
PP PC	Dipalmitoyl phosphatidylcholine
PP PG	Dipalmitoyl phosphatidylglycerol
PS	Phosphatidylserine
ROE	Reorientation enzyme
RP	Reverse phase
SDS-PAGE	Sodium dodecyl sulphate-polyacrylamide gel electrophoresis
SEC	Size exclusion chromatography
SM	Sphingomyelin
sPLA2	Secretory phospholipase A2
SUVs	Small unilamellar vesicles
TA	Transacylase
TAG	Triacylglycerol
TLC	Thin layer chromatography

Tris	Tris(hydroxymethyl)aminomethane
UPLC	Ultra high performance liquid chromatography
VLDL	Very low density lipoprotein

LIST OF APPENDICES

Appendix A- Supplementary Methods

Appendix B- Supplementary Results

BIOSINTESIS LIPID ENDOSOM-SPESTIFIK BIS(MONOASILGLISERO)FOSFAT

ABSTRAK

Hipotesis menyatakan laluan biosintetik *de novo* endosom-spesifik bis(monoasilglisero)fosfat (BMP) daripada perintis fosfatidylgliserol (PG) endogen melalui perantara lysofosfatidylgliserol (LPG) telah dipertimbangkan. Dalam kajian ini, laluan biosintetik alternatif BMP daripada PG melalui perantara asilfosfatidylgliserol (AcPG) dicadangkan. Suatu kuantiti AcPG yang agak ketara didapati berada dalam dan luar sel sepanjang 24 jam pengeraman dengan PG eksogen. Enzim transasilase adalah diperlukan untuk memindah suatu rantai asil daripada penderma PG kepada penerima PG, maka menukarkan penerima PG kepada AcPG dan penderma PG kepada LPG. Untuk melengkapkan biosintesis BMP yang melibatkan laluan AcPG, langkah orientasi semula moiety gliserol dwi-asil mesti berlaku seiring dengan kehilangan sisa asil. Cadangan laluan penukaran PG kepada BMP melalui aktiviti transasilase yang menghasilkan AcPG telah disahkan melalui assai *in vitro* dengan menggunakan serum foetal bovin (FBS). Aktiviti transasilase yang menyerupai fosfolipase A1 dikenalpasti dengan menggunakan PO PG yang tidak simetri sebagai penerima dan penderma, maka menghasilkan PO-P AcPG : PO-O AcPG pada nisbah 10:1. Selanjutnya, aktiviti transasilase dicirikan dari segi ion dwivalen, pH dan spesifikasi substrat. Eksperimen-eksperimen *in vitro* menggunakan koktel enzim yang dirembes daripada sel RAW 264.7 dalam keadaan kebuluran menunjukkan kehadiran kedua-dua aktiviti enzim yang dicadangkan, aktiviti transasilase dan orientasi semula. Pada masa pertengahan, jumlah kuantiti PG, BMP dan AcPG adalah kurang secara ketara berbanding dengan kuantiti PG yang dibekalkan pada masa permulaan atau jumlah BMP yang dihasilkan selepas

pengeraman selama 24 jam. Peningkatan kuantiti TAG dalam sel menandakan PG boleh ditukarkan kepada TAG melalui DAG untuk menyimpan asid-asid lemak berlebihan yang disalurkan kepada sel. Pada peringkat yang seterusnya, sebahagian TAG digunakan untuk sintesis *de novo* BMP. Langkah-langkah pemecahan yang bersiri telah dikenalpasti untuk menuliskan aktiviti transasilase daripada FBS, bermula daripada pemendakan ammonium sulfat, kromatografi turus oktil sefaros dan Q sefaros. Identiti protein daripada pecahan yang diperkaya dengan aktiviti transasilase dilakukan melalui analisis proteomik LC-MS dan perbandingan berdasarkan database bovin dilakukan. Calon protein yang teramat dikenalpasti sebagai vanin 1 dan berberat molekul ialah 56.9 kDa. Secara menariknya, analisis proteomik supernatan sel RAW 264.7 dalam keadaan kebuluran menunjukkan kehadiran sekumpulan lipase yang dirembes, seperti fosfolipase A2, fosfolipase C dan fosfolipase D.

BIOSYNTHESIS OF ENDOSOME-SPECIFIC LIPID BIS(MONOACYLGLYCERO)PHOSPHATE

ABSTRACT

The hypothetical *de novo* biosynthetic pathway of endosome-specific phospholipid, bis(monoacylglycero)phosphate (BMP) from endogenous phosphatidylglycerol (PG) precursor via lysophosphatidylglycerol (LPG) intermediate had been considered. In the present study, an alternative BMP biosynthetic route from PG via acylphosphatidylglycerol (AcPG) intermediate was proposed. A considerable amount of AcPG was found present in and outside the RAW 264.7 cells during 24 hours of incubation with exogenous PG. A transacylase is required to transfer an acyl chain from a PG donor to a PG acceptor, transforming the acceptor PG into AcPG and the donor PG into LPG. To complete the BMP biosynthesis following the AcPG route, a reorientation step of the diacylated glycerol moiety has to occur with concomitant loss of an acyl residue. The new pathway of PG conversion to BMP via AcPG forming transacylase activity was established by an original *in vitro* assay utilizing fetal bovine serum (FBS) as enzymatic source. A phospholipase A1 displaying a transacylase activity was revealed by utilizing asymmetric PO PG as acceptor and donor, yielding a PO-P AcPG:PO-O AcPG ratio of 10:1. This transacylase activity was further characterized in terms of divalent ions, pH and substrate specificity. *In vitro* experiments utilizing the secreted enzyme complex from RAW 264.7 cells grown under starvation conditions indicated that both proposed enzymatic activities, transacylase and reorientation, were present. At intermediate time points, the combined amount of PG, BMP and AcPG was significantly less compared to the amount of supplied PG at the beginning or the total BMP amount produced after 24 hours of incubation. An elevation in triacylglycerol

amount in the cell after 8 hours of incubation indicated that PG could be converted to triacylglycerol via diacylglycerol to store temporarily the excessive amount of fatty acids provided to the cells. At a later stage, a part of the stored triacylglycerol is used for the *de novo* synthesis of BMP. Fractionation steps were established to purify the extracellular transacylase activity from FBS, using ammonium sulfate precipitation, octyl sepharose and Q sepharose column chromatography. Protein identification of the fractions enriched with transacylase activity was performed by LC-MS proteomics analysis and matched against a bovine database. The most potent candidate protein was identified as vanin 1 with a molecular weight of 56.9 kDa. Interestingly, proteomics analysis of the supernatant of starved RAW 264.7 cells disclosed the presence of a pool of secreted lipases such as phospholipase A2, phospholipase C and phospholipase D.

CHAPTER 1

LITERATURE REVIEW

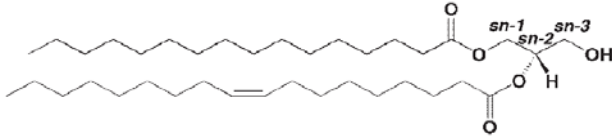
1.1 Lipid overview

Lipids are naturally occurring organic compounds which are soluble in organic solvent but are immiscible in water (Fahy *et al.*, 2005). Lipids are often referred to as fat if their physical appearance at room temperature is solid and called oil if it is liquid (Kent, 2000; Caballero, 2006). Lipids are distinct from proteins, carbohydrates and nucleic acids with respect to the incredible heterogeneity of their molecular structure. In principle, cellular metabolites are categorized predominantly according to their solubility as lipids rather than due to specific structural features (O'Keefe, 2002; Fahy *et al.*, 2005; Stoffel, 2012). As lipids are at the intersection of biology and chemistry, an unambiguously nomenclature suitable for both fields is important. Consequently, lipid nomenclature is jointly defined by the International Union of Pure and Applied Chemistry (IUPAC) and International Union of Biochemistry and Molecular Biology (IUBMB) and outlined at <http://www.chem.qmul.ac.uk/iupac/> website (Fahy *et al.*, 2005; Fahy *et al.*, 2009).

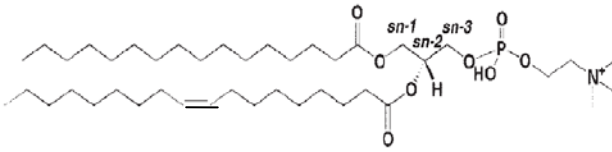
Lipids are categorized into eight major classes, including fatty acyls/fatty acids, glycerolipids, glycerophospholipids, sphingolipids, sterol lipids, prenol lipids, saccharolipids and polyketides. The representative structure for each of the lipid class is depicted in figure 1.1. While fatty acids exhibit limited complexity, polyketides, sterols and saccharolipids exhibit a significant level of complexity.



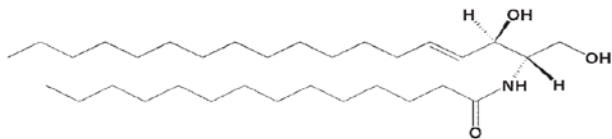
(1) Fatty acids: hexadecanoic acid



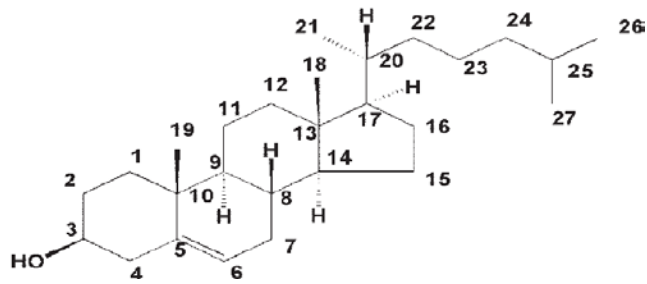
(2) Glycerolipids: 1-hexadecanoyl-2-(9Z-octadecenoyl)-*sn*-glycerol



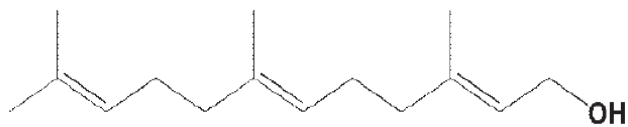
(3) Glycerophospholipids: 1-hexadecanoyl-2-(9Z-octadecenoyl)-*sn*-glycero-3-phosphocholine



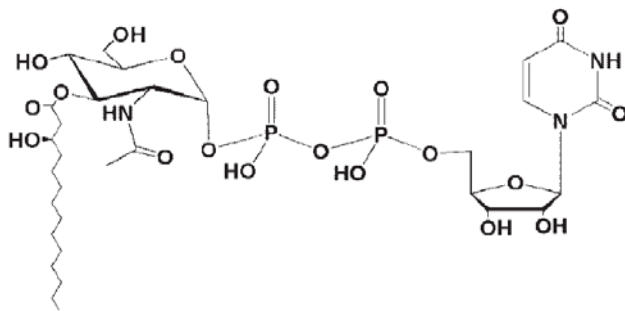
(4) Sphingolipids: N-(tetradecanoyl)-sphing-4-enine



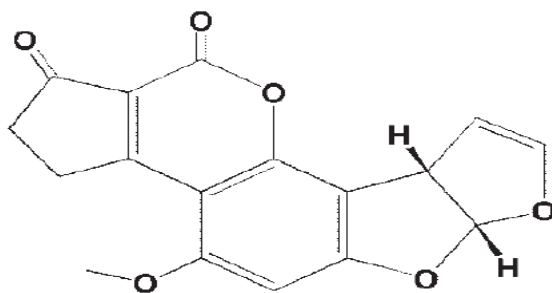
(5) Sterol lipids: cholest-5-en-3 β -ol



(6) Prenol lipids: 2E, 6E-farnesol



(7) Saccharolipids: UDP-3-O-(3R-hydroxy-Tetradecanoyl)- α D-N-acetylglucosamine



(8) Polyketides: aflatoxin B1

Figure 1.1: Representative structure for each of the lipid classes (Fahy *et al.*, 2005)

Based on the lipid nomenclature as defined by the IUPAC-IUBMB, it is noteworthy to highlight few key features relevant to this study as follows:

1. The stereospecific numbering (*sn*) is applied to describe glycerolipids and glycerophospholipids. Commonly, the *sn*-1 and/or *sn*-2 position are acylated, while the *sn*-3 position is phosphorylated in mammalian and bacterial glycerolipids.
2. The employment of *R/S* nomenclature (as opposed to α/β) is utilized to emphasize difference in the stereochemical configuration of the glycerol backbone.
3. The common term “lyso”, implying that one of the acyl/alkyl groups is not present in glycerolipids and glycerophospholipids, it will not be utilized in systematic names, but will be included as a synonym to improve readability (Moss, 1976; Fahy *et al.*, 2005).

The definition of stereospecific numbering is as follows: The carbon atom at the top in the Fischer projection of the glycerol backbone with the hydroxyl group at carbon-2 pointing to the left is designated as C-1. To distinguish stereospecific numbering from conventional numbering lacking steric information, the prefix “*sn*” is used. Importantly, the use of stereospecific numbering is only limited to glycerolipids and glycerophospholipids (Moss, 1976).

In general, each carbon atom with different substituent is considered a chiral center. A chiral molecule can have one or more chiral centers. A molecule with multiple chiral centers is a chiral if it is not superimposable with its mirror image. Two molecules which are the exact mirror image of each other are considered enantiomer. To clearly define the molecular structure in a standardized manner,

Cahn-Ingold-Prelog (CIP) rule should be applied to differentiate between R and S configuration of the stereocenter under consideration. The steps are:

1. The order of the substituents is according to the priority from 1 to 4 (or 'a' to 'd' as shown in the example below), with 1 assigned to the substituent with the highest molecular weight, and 4 with the lowest. Break ties by taking substituents of equal atoms in a stepwise procedure into consideration.
2. Rotate the molecules so that the substituent of lowest molecular weight is facing away from you, thus the molecule is viewed down the bond from the chiral center to the lowest priority group.
3. The handedness is assigned based on the sequence of priority read around the chiral carbon atom. If the priority of the atoms from 1-3 is read in a counterclockwise direction, the chiral carbon atom is considered left handed and named as S enantiomer. S stands for 'sinister', meaning in Latin is left. If the priority of the atoms from 1-3 are read in a clockwise direction, the center is considered right handed and named as R enantiomer. R stands for 'rectus', meaning in Latin is right.

A practical example how to determine S and R enantiomers is shown in figure 1.2 (Willock, 2009).

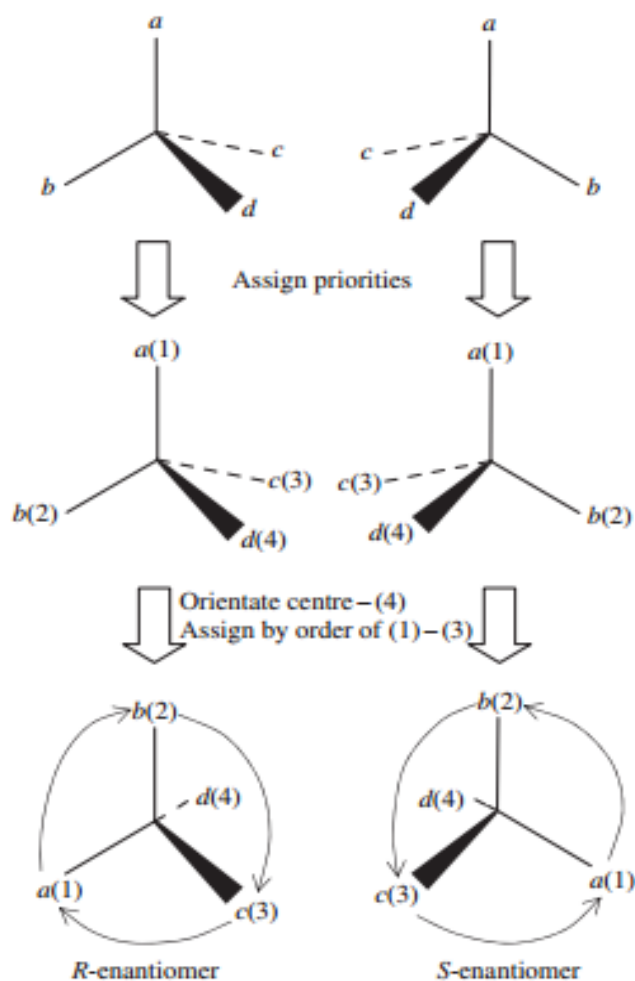


Figure 1.2: Assignment of S and R enantiomers following CIP rules. In this example the priority groups are read $a > b > c > d$ (Willock, 2009)

Commonly, lipid structures tend to be drawn from left to right. In case of simple fatty acids or prenol building blocks, the acid carboxyl or hydroxyl group is thus drawn on the right and the hydrophobic hydrocarbon tail is drawn on the left, as shown in figure 1.1. Similarly, in glycerolipids and glycerophospholipids, the hydrocarbon chains tend to be drawn on the left and the glycerol moiety is drawn horizontally, similar to Fischer projection, providing direct visualization of the stereochemistry (if known). In contrast to glycerophospholipids, sphingolipids lack a glycerol moiety. Nonetheless, the head groups of glycerophospholipids and sphingolipids tend to be depicted on the right and the hydrocarbon tails tend to be

depicted on the left. Inevitably, structurally complex lipids cannot adhere to this common guideline, such as sterol, saccharolipids and polyketides (Fahy *et al.*, 2005). Nevertheless, liberal exception can and will be applied throughout this dissertation.

To support advances in lipid biology and lipidomics large repertoires such as LIPIDAT and Lipid Bank have been established. LIPIDAT and Lipid Bank provide catalog, annotation and functional classification of lipids (Fahy *et al.*, 2005).

Lipids serve as the primary energy storage in living organisms by supplying more than twice the energy per gram compared to carbohydrates (van Meer *et al.*, 2008). In addition, lipids function as heat insulation, shock absorption and buoyancy (Kent, 2000). Lipids play crucial roles as mediators for signal transmission in many cellular pathways. Lipids are also involved in cell differentiation as well as hormone and cytokine synthesis (Caballero, 2006; Eyster, 2007).

Fatty acids are the simplest molecules among lipids. Their structure and nomenclature are illustrated in figure 1.3 and table 1.1, respectively (Fahy *et al.*, 2005).

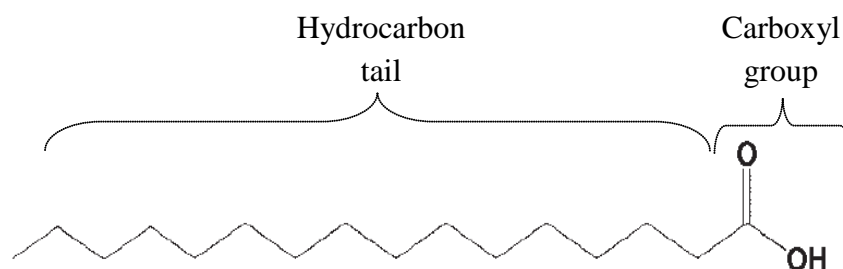


Figure 1.3: Structure of a fatty acid chain which consists of a carboxyl head group and a hydrocarbon tail (Fahy *et al.*, 2005)

Table 1.1 Physiologically relevant fatty acids (Fahy *et al.*, 2005)

Number of carbons	Number of double bonds	Numerical Symbol/ Shorthand	Common name
14	0	14:0	Myristic acid/ Myristate
16	0	16:0	Palmitic acid/ Palmitate
16	1	16:1 ^{Δ⁹}	Palmitoleic acid/ Palmitoleate
18	0	18:0	Stearic acid/ Stearate
18	1	18:1 ^{Δ⁹}	Oleic acid/ Oleate
18	2	18:2 ^{Δ^{9,12}}	Linoleic acid/ Linoleate
18	3	18:3 ^{Δ^{9,12,15}}	α-Linolenic acid (ALA)/ Linolenate
20	4	20:4 ^{Δ^{5,8,11,14}}	Arachidonic acid/ Arachidonate
20	5	20:5 ^{Δ^{5,8,11,14,17}}	Eicosapentaenoic acid (EPA)
22	6	22:6 ^{Δ^{4,7,10,13,16,19}}	Docosahexaenoic acid (DHA)

Note: The position of double bonds is indicated by Δ^n , where n indicates lower numbered carbon of each pair.

Most mammalian fatty acids have an even number of carbon atoms and ranging between 12-22 carbons. DHA is an example of a common polyunsaturated fatty acid. In general, fatty acids are denoted by a numerical symbol or shorthand description, as shown in table 1.1. For example, 18:1 for oleic acid which implies 18 carbon atoms and 1 double bond in the acid chain, commonly at position delta 9. The non polar hydrocarbon chain and the polar carboxyl group confer the amphipathic

nature of lipids, resulting in the spontaneous self assembly of lipids and the formation of small vesicular or lamellar arrangements in aqueous environment (van Meer *et al.*, 2008; Bohdanowicz and Grinstein, 2013). Not all lipids exhibit polar amphipathic nature. For example, the uncharged neutral lipids include fatty acid esters (carbon atom more than 12), mono-, di-, triacylglycerols, sterols, sterol esters and prenols (O'Keefe, 2002).

Liposomes are artificial vesicles that exhibit a phospholipid bilayer arrangement, mimicking the biological membrane up to a certain degree. Importantly, the lipid composition can be changed easily according to the experimental design. Figure 1.4 displays the schematic illustration of liposomes of different sizes, including small unilamellar vesicle (SUV), large unilamellar vesicle (LUV), multilamellar vesicle (MLV) and multivesicular vesicle (MVV). The liposomal sizes of SUV and LUV are 20-100 nm and 100-400 nm, respectively. Whereas the liposomal sizes of MLV and MVV fall in the range of 200 nm to approximately 3000 μm .

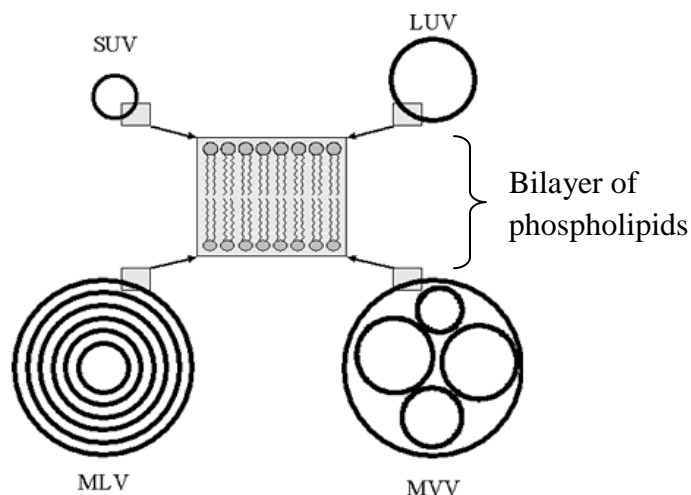


Figure 1.4: Schematic illustration of liposomes of different sizes, including small unilamellar vesicle (SUV), large unilamellar vesicle (LUV), multilamellar vesicle (MLV) and multivesicular vesicle (MVV) (<http://www.azonano.com/article.aspx?ArticleID=1243>)

1.2 Membrane phospholipids

The fluid mosaic model of the structure of cell membranes proposed by Singer and Nicolson was the first step towards a better understanding of the importance of lipids and has been widely accepted (Singer and Nicolson, 1972). Lipids, proteins and carbohydrates are the biological molecules which form the architecture of the plasma membranes. At the most rudimentary level, the cell membrane is constituted of a lipid bilayer with the polar hydrophilic head of each lipid molecule facing either towards the cytoplasm or extracellular matrix, while their hydrophobic tails face towards each other. Integral membrane proteins are embedded in this membrane bilayer, while peripheral proteins form transient interactions with lipid bilayer. Carbohydrates are either covalently attached to the protein as glycoproteins or to lipids as glycolipids (saccharolipids) and are involved in cellular physiology (Singer and Nicolson, 1972; Eyster, 2007).

The lipid composition of each subcellular organelle and the plasma membrane varies according to the specific task performed at each of the subcellular compartment. For instances, plasma membranes are enriched in sterols and sphingolipids, less abundant in phospholipids in order to confer mechanical strength to the cells (van Meer *et al.*, 2008). The heterogeneous distribution of lipids and proteins over the membranes and the spatial and temporal lipid-protein interaction attributed to the function of membranes in living cells (Smith, 2012). Lipid-lipid immiscibility results in lateral heterogeneity of the membrane leaflet, often called lipid raft. Lipid rafts or microdomains are broadly defined as liquid-ordered membrane domains in which the lipids are more tightly packed compared to the surrounding non-raft bilayer. The high packing of raft is due to the saturated hydrocarbon chains in raft phospholipids and sphingolipids (Rajendran and Simons, 2005).

Glycerophospholipids or in short, phospholipids are one of the main constituents of all cell membranes displaying a great diversity (Hermansson *et al.*, 2011). Phospholipids constitute the bulk of the cellular membrane lipids, including phosphatidic acid (PA), phosphatidylcholine (PC), phosphatidylethanolamine (PE), phosphatidylserine (PS), phosphatidylglycerol (PG), phosphatidylinositol (PI), cardiolipin (CL), lysophosphatidic acid (LPA) and lysobisphosphatidic acid (LBPA), also known as bis(monoacylglycero)phosphate (BMP) (van Meer *et al.*, 2008). The amphipathic nature of phospholipids allows cells and subcellular organelles to be separated or compartmentalized by membranes. Lipid membranes act not merely as highly selective physical barrier in and between cells, but play a central role in numerous metabolic processes (Escriba *et al.*, 2008; van Meer *et al.*, 2008). Figure 1.5 displays the representative structure of common phospholipids. The glycerol

backbone of phospholipids (as outlined with green box) is usually esterified with two fatty acyl chains at *sn*-1 and *sn*-2 position, respectively (highlighted by a purple box). The head group (represented by “X”) is linked via a phosphate residue (outlined with a blue box) to the *sn*-3 position of the glycerol backbone. The head group of phospholipids gives rise to the name of each phospholipid. The phospholipids shown in figure 1.5 encompass PA, PC (also called lecithin), PE, PS, PI and PG (Kelly and Jacobs, 2016). Two letter abbreviations are commonly used to identify phospholipid subclasses.

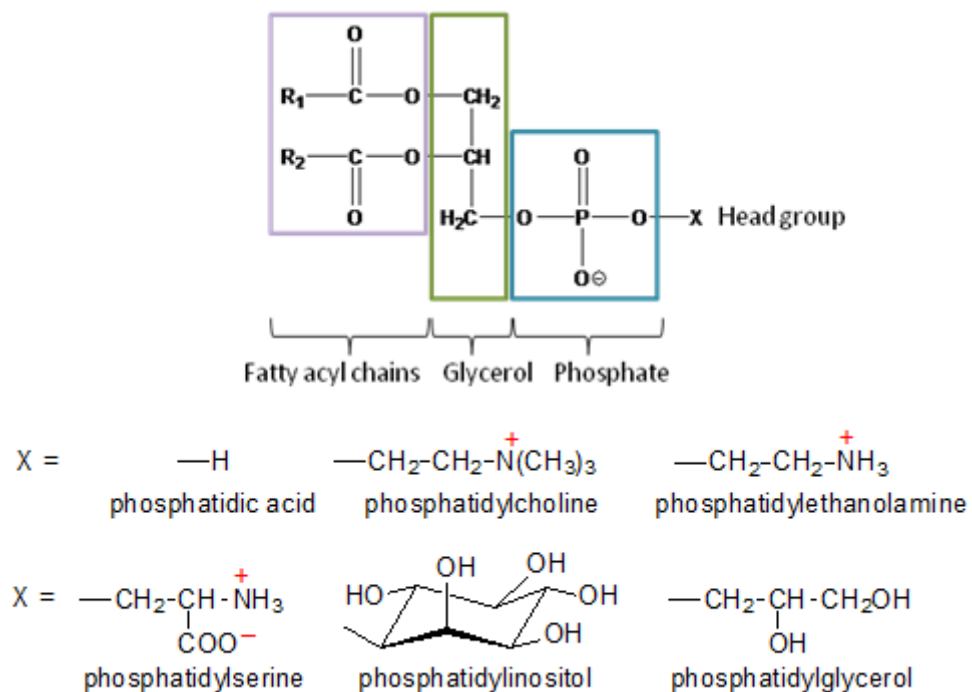


Figure 1.5: Representative structures of common phospholipids (Kelly and Jacobs, 2016)

1.3 Biosynthesis of phospholipids

Lipids are produced, transported, recognized and degraded by a variety of enzymes, binding proteins and receptors (Fahy *et al.*, 2005). Within the eukaryotic

cells, the synthesis of a particular lipid is often organelle-specific. The endoplasmic reticulum (ER) is the primary location for the synthesis of a large number of lipids such as functional phospholipids and cholesterol. CL and BMP are considered exclusively synthesized in the mitochondrial and endosomal membrane, respectively. Triacylglycerol (TAG) and cholesteryl ester (CE) are produced at the ER. Sphingolipid synthesis is completed in the Golgi apparatus. As phospholipids and sphingolipids are found in all cellular membranes, these lipids have to be exported from their site of synthesis to their target organelles, requiring an efficient packing and sorting mechanism. The Golgi apparatus acts as the major lipid sorting site (van Meer *et al.*, 2008).

The biosynthesis of the main constituents of the phospholipid membrane is very different between archaea, bacteria and eukaryotes, as deciphered in figure 1.6 (Lombard *et al.*, 2012).

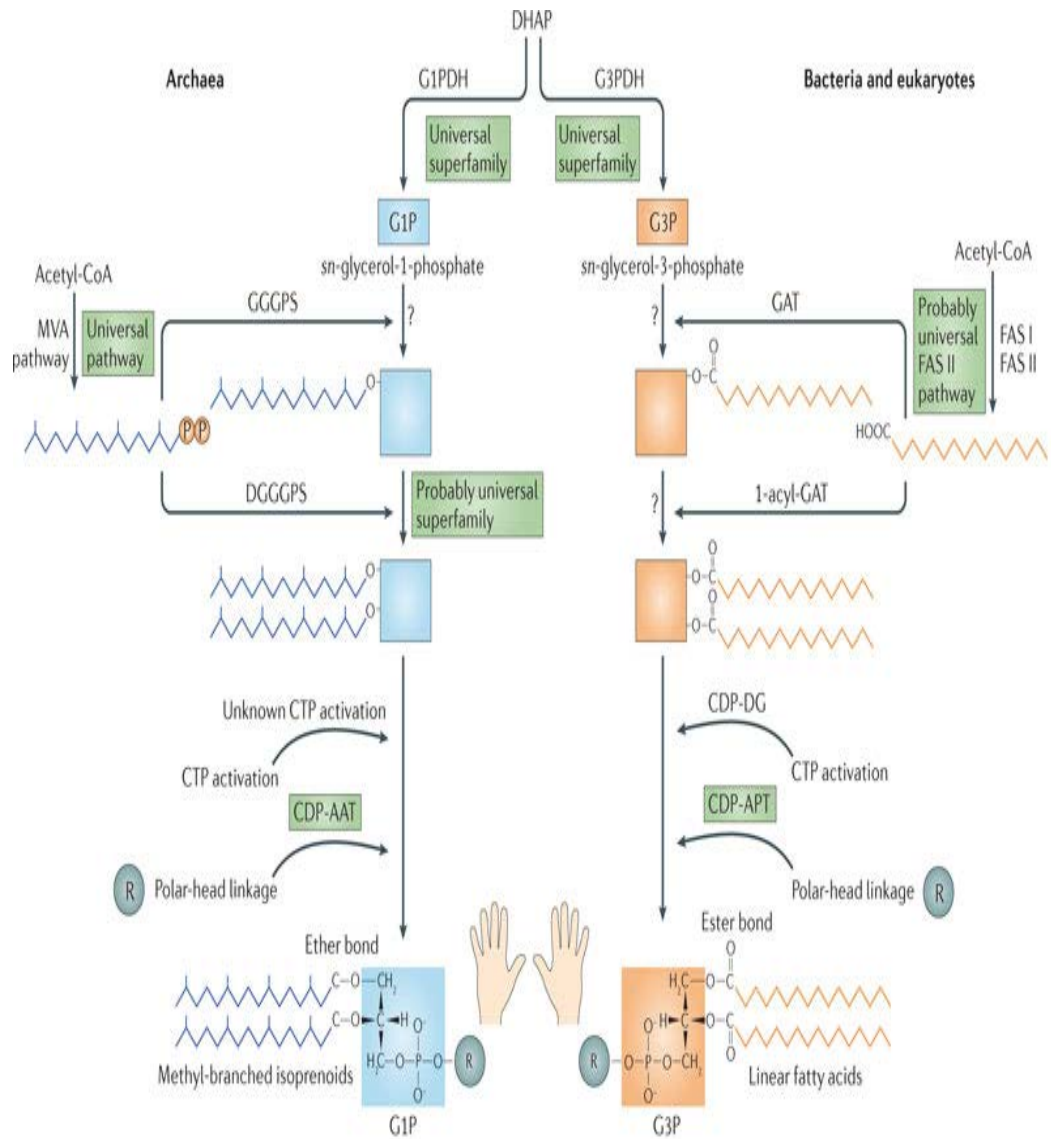


Figure 1.6: Comparison of the biosynthetic pathways of phospholipids in archaea, bacteria and eukaryotes (Lombard *et al.*, 2012)

In bacteria and eukaryotes, phospholipids are composed of glycerol-3-phosphate (G3P) derivatives. On contrary, phospholipids in archaeal membrane are derived from glycerol-1-phosphate (G1P) (Lombard *et al.*, 2012). The stereoconfiguration of the glycerophosphoglycerol backbone has attracted special interest due to its cellular physiological roles and involvement in the evolution of life (Taniguchi *et al.*, 2015). The protein-phospholipid interaction is based on electrostatic interaction, which in turn strongly depends on the actual stereoconfiguration of both chiral partners. While some phospholipids act as substrate, requiring a key-lock type interaction with special emphasize on their stereoconfiguration, others act as ligands during signaling processes or are functional independent of their interaction with proteins (Bohdanowicz and Grinstein, 2013).

The phospholipid BMP, the main focus of this dissertation is primarily of eukaryotic origin. Consequently, BMP is derived from a G3P precursor. Therefore, special emphasis will be put on the biosynthesis of phospholipids derived from G3P.

1.4 Bis(monoacylglycero)phosphate (BMP)

1.4.1 Structure and *de novo* biosynthesis of BMP

The structure of BMP is depicted in figure 1.7. BMP features a glycerophosphoglycerol backbone and both of the glycerol moieties are esterified to the central phosphate residue at carbon number-1. Consequently, the BMP backbone is featuring a stereoconfiguration number (*sn*) of *sn*-1,1' diglycerophosphate that was confirmed recently (Brotherus *et al.*, 1974; Jouti *et al.*, 1976; Jouti and Renkonen, 1979; Tan *et al.*, 2012). The absence of any cationic charge renders BMP an anionic phospholipid, carrying a negative charge on its phosphate head group. Additionally,

each side of the glycerol is esterified with a single acyl chain. The length of the acyl chains and their saturation degree vary according to the cell type. In cultured mammalian cells, the main acyl chain species of BMP is oleic acid, featuring 18 carbon atoms and a double bond (18:1) (Mason *et al.*, 1972; Brotherus and Renkonen, 1974; Huterer and Wherrett, 1979; Cochran *et al.*, 1985; Kobayashi *et al.*, 2002; Akgoc *et al.*, 2015). The exact location of the acyl chains on both of the glycerol moieties of natural BMP is still unclear (Wherrett and Huterer, 1973; Amidon *et al.*, 1996).

BMP is a peculiar mammalian phospholipid exclusively displaying an *sn*-1,1' diglycerophosphate backbone, resembling the phospholipids of the archaeal domain (Tan *et al.*, 2012). The unique stereoconfiguration is likely one of the reasons why BMP exhibits a considerable stability under the highly acidic lysosomal environment, which is rich in lytic enzymes (Appelqvist *et al.*, 2013). In general, the lysosomes are regarded as the digestive stomach of cell, based on their ability to digest cellular metabolites, such as proteins, nucleotides and lipids into their building blocks (Schulze *et al.*, 2009). Not surprisingly, BMP has been reported to be resistant against degradation by phospholipases (Matsuzawa and Hostetler, 1979). The turnover of the BMP backbone is much slower than the turnover of its acyl chains, particularly in case of polyunsaturated fatty acids (Huterer and Wherrett, 1990). The unusual stereoconfiguration of BMP reflects its unique physiological roles and likewise, its biosynthesis must differ considerably from other phospholipids of mammalian origin.

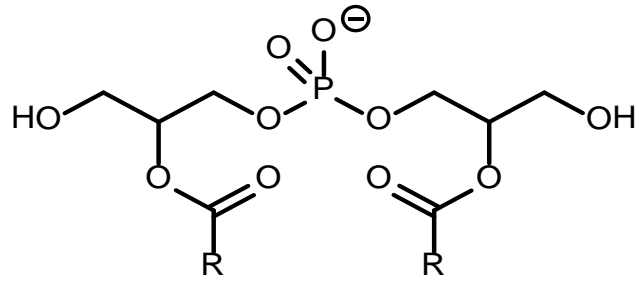


Figure 1.7: Stereoconfiguration of BMP: *sn*-1,1' diglycerophosphate

LPA formation is the first step from G3P during the *de novo* biosynthesis of mammalian phospholipids. Next, LPA is converted to PA by a LPA acyltransferase (AGPAT, also known as LPAAT), a short lived key intermediate in phospholipid biosynthesis. PA is mainly metabolized into two types of glycerol derivatives. Firstly, diacylglycerol (DAG), which is converted to TAG, PC, and PE. PS in turn is synthesized from PC or PE. Secondly, cytidine diphosphate-diacylglycerol (CDP-DAG) is processed into PI, PG, CL, and BMP. The *de novo* biosynthesis of BMP from PA is depicted in figure 1.8, involving CDP-DAG synthase, phosphatidylglycerophosphate (PGP) synthase and PGP phosphatase.

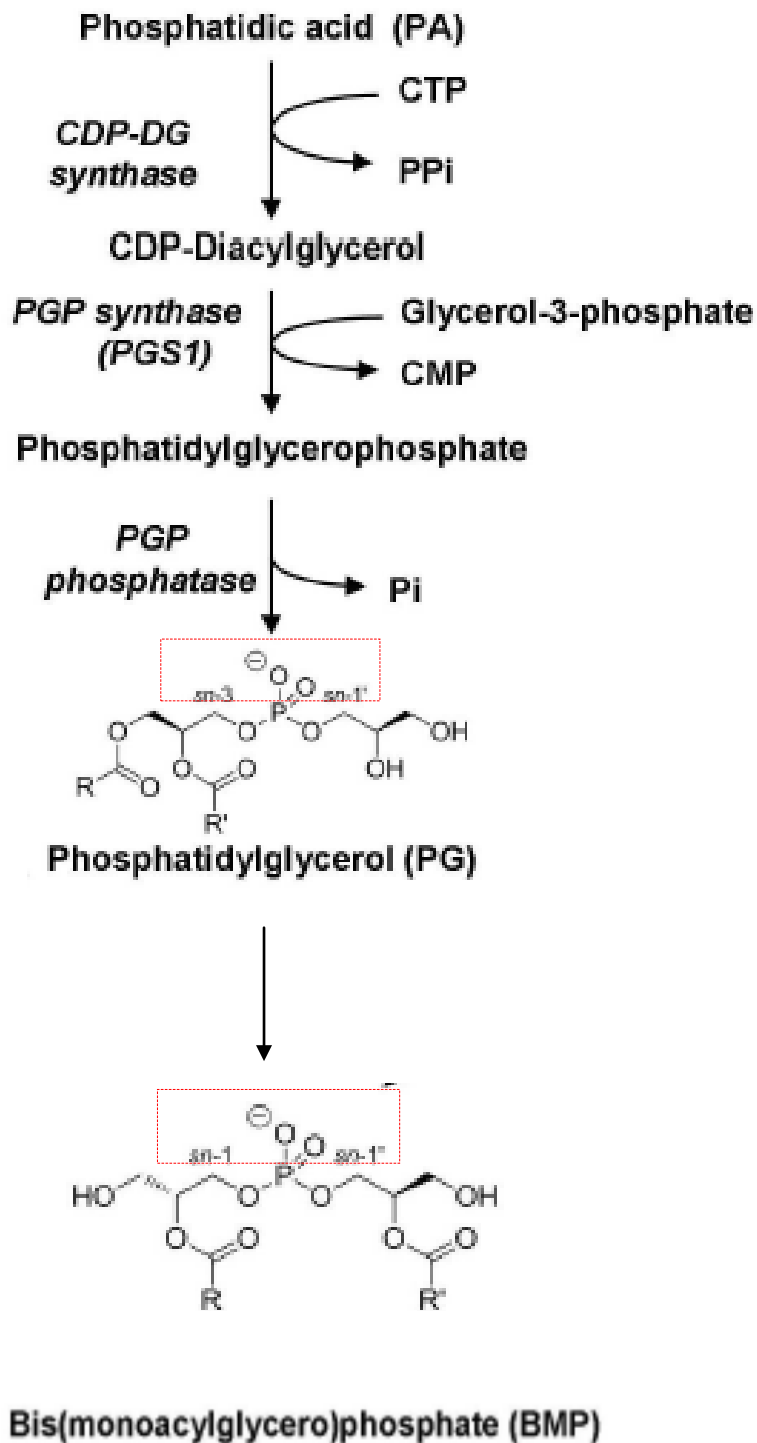


Figure 1.8: The *de novo* biosynthesis of BMP from PA. The enzymes catalysing the successive steps from PG to BMP have not been characterized yet. Red squares indicate the altered backbone configuration between PG and BMP

Special attention should be paid to the backbone of PG and BMP which is highlighted in red dotted line as shown in figure 1.8. The backbone of naturally occurring PG is *sn*-3,1' diglycerophosphate. Notably, BMP exhibits an *sn*-1,1' diglycerophosphate backbone (Hullin-Matsuda *et al.*, 2009). Nevertheless, BMP is not just a simple structural isomer of PG and the conversion of PG to BMP is not a straight forward process (Thornburg *et al.*, 1991; Hullin-Matsuda *et al.*, 2014). Extended scientific interest and discussion clarified that the reorientation of the glycerol backbone of PG precursor or more likely one of the synthesis intermediates is the key step leading to the biosynthesis of BMP with its unusual stereoconfiguration (Somharju and Renkonen, 1980; Frentzen-Bertrams and Debuch, 1981; Amidon *et al.*, 1995). To-date it is not clear whether the mechanism resulting in glycerol backbone reorientation is facilitated by a single or a set of enzymes (Thornburg *et al.*, 1991).

1.4.2 Cellular localization and biological roles of BMP

BMP is an endosome-specific phospholipid which is found primarily in the late endosomal and lysosomal organelles of mammalian cells (Kobayashi *et al.*, 1998). BMP is highly enriched in the internal membranes of late endosomes accounting for up to 15 % of total late endosomal phospholipids (Kobayashi *et al.*, 2002; Hullin-Matsuda *et al.*, 2009). BMP content, which is less than 1 % of total cellular phospholipids, strongly depends on the culture conditions and cell line or tissue types (Frederick *et al.*, 2009; Akgoc *et al.*, 2015). Late endosomes play a decisive role for incoming material in the endocytic pathway and outgoing components to the lysosomes, the Golgi complex or the plasma membrane, as shown in figure 1.9 (Scott *et al.*, 2014). Endocytosis is the general term defined as the

internalization process of solutes, fluid, macromolecules and plasma membrane components. The endocytosis mechanism is initiated by plasma membrane invagination, followed by membrane fission, budding off the membrane and transport of the resulting vesicle via early endosomes, multivesicular bodies to late endosomes, and finally lysosomes (Huotari and Helenius, 2011).

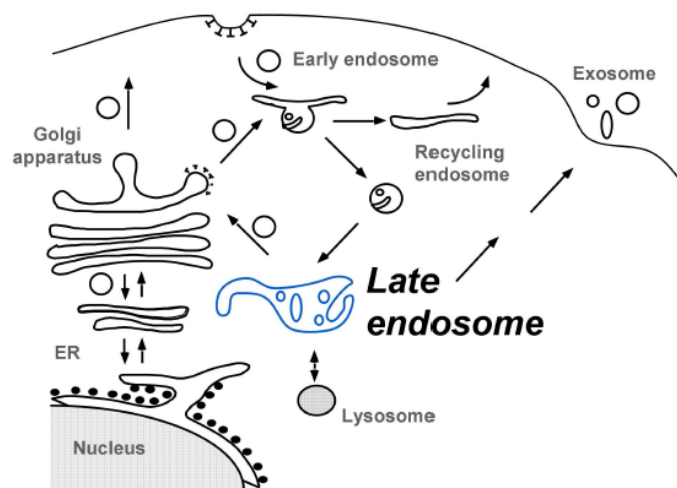


Figure 1.9: Endocytosis via early endosome, late endosome and lysosome (Scott *et al.*, 2014)

Mounting evidence indicates that BMP-rich domains play a crucial role during cholesterol homeostasis and glycolipids degradation in late endosomes (Chevallier *et al.*, 2008; Schulze *et al.*, 2009). BMP is involved in the lipid and protein transport within the endosomal system after their delivery via endocytosis or autophagy (Kobayashi and Hirabayashi, 2000; Hullin-Matsuda *et al.*, 2009). Additionally, BMP is involved in the formation of the archetypal multivesicular bodies during the endosomal maturation. These internal membranes are rich in BMP and are considered to exhibit specific properties favoring digestion based on the physical properties of BMP. Additionally, BMP provides structural organization for

formation and stability of multivesicular bodies (Frederick *et al.*, 2009; Kolter and Sandhoff, 2010).

1.4.3 Proposed biosynthetic pathway of BMP from PG

1.4.3(a) Phospholipase and transacylase

Hydrolases are an important class of enzymes and represent a significant proportion of cellular proteins. They are generally implicated in degradative process but also in many physiological processes, such as signaling. Utilizing a molecule of water as acceptor, hydrolases cleave carbon-hetero atom bonds such as esters, ethers and acetyls. Depending on substrate specificity, hydrolases are subcategorized into nucleases (nucleic acids), proteases (proteins), glycosidases (carbohydrates or sugars), phosphatases (phosphate esters) and lipases (lipids). Additionally, hydrolases can be classified according to the functional group affected, such as carbon ester hydrolases, phosphate ester hydrolases, pyrophosphate ester hydrolases, phosphodiester hydrolases and amide hydrolases (Dennis, 2015).

The first step involved in the biosynthetic pathway of BMP from its PG precursor is the cleavage of the *sn*-2 acyl chain of PG by a phospholipase (PLA) (Waite *et al.*, 1990; Amidon *et al.*, 1995). Phospholipases belong to the large group of hydrolases and catalyze the hydrolysis of acyl esters (acyl hydrolases) or phosphate esters (phosphodiesterase) on phospholipids (Dennis, 2015). Phospholipases are further classified according to the position they hydrolyze on the phospholipid backbone. Phospholipase A1 (PLA1), phospholipase A2 (PLA2), phospholipase B (PLB) and lysophospholipase A1/2 (lysoPLA1/2) are the acyl hydrolases, whereas phospholipase C (PLC) and phospholipase D (PLD) constitute

the phosphodiesterases, as shown in figure 1.10. PLA1, PLA2 and PLC cleave the ester bonds connecting to carbon at *sn*-1, *sn*-2 or *sn*-3 position, respectively. PLD catalyzes the hydrolysis of phospholipids at the phosphodiester bond, adjacent to the PLC sensitive phosphate ester bond. PLB hydrolyzes both the *sn*-1 and *sn*-2 ester bonds, while lysoPLA1/2 can be either specific for the *sn*-1 or *sn*-2 ester bond or cleave both with same affinity, but in any case they utilize only lysophospholipids as substrate (Richmond and Smith, 2011).

Phospholipases are ubiquitously expressed in all tissues and take a variety of forms, such as soluble proteins usually secreted from cells, membrane associated or restrained to specific intracellular compartments. While some require cofactors for activity, others are activated at specific pH environment. Phospholipases exhibit large variety of functions and can be categorized into three main functions: (1) as digestive enzymes breaking down phospholipids and thus regulating the turnover of phospholipids; (2) as phospholipases responsible to maintain membrane integrity by acyl remodeling. The exchange of acyl chains between phospholipids occurs frequently in living cells and is catalyzed by acyl hydrolases or acyltransferases. Consequently, transfer of acyl chains between phospholipids increases phospholipid diversity and can play a decisive role in cellular physiological pathways; (3) as phospholipases contributing to the production of bioactive lipid mediators, such as for signal transduction. Among phospholipases, PLA2, PLC and PLD are the most established lipases involved in the formation of bioactive lipid molecules (Richmond and Smith, 2011).

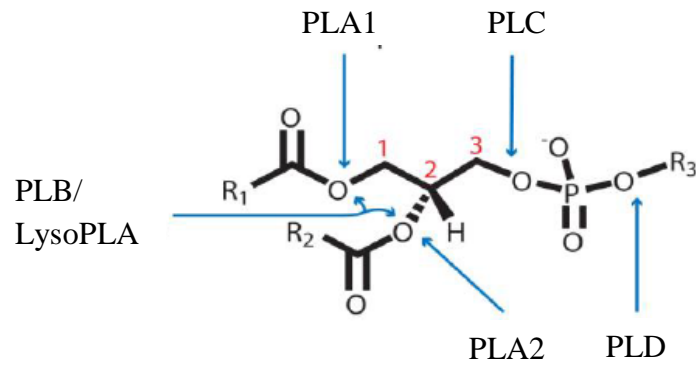


Figure 1.10: Ester bond specificity of phospholipases (Richmond and Smith, 2011)

In addition to phospholipase-dependent hydrolysis, acylation takes place during the biosynthesis of BMP from PG and is catalyzed by transacylase (TA) and acyltransferase. Transacylase is generally defined as the enzyme catalyzing the transfer of acyl groups esterified in phospholipids to lysophospholipids without the generation of free fatty acids (Yamashita *et al.*, 1997; Yamashita *et al.*, 2014). Transacylases are CoA-dependent or CoA-independent. Acyltransferase catalyzes the transfer of an acyl group from an acyl-CoA to any of various acceptors (Shindou and Shimizu, 2009; Hishikawa *et al.*, 2014; Yamashita *et al.*, 2014).

The proposed pathway for the biosynthesis of BMP from PG is shown in figure 1.11. A PLA2 cleaves the *sn*-2 acyl chain of PG (as highlighted in the green box) to form *sn*-3:*sn*-1'LPG (step 1). Next, LPG is acylated at the head group glycerol by a transacylase, using a phospholipid as the acyl donor to form *sn*-3:*sn*-1'BMP (step 2). Subsequently, the backbone of BMP is reoriented from *sn*-3:*sn*-1'BMP to *sn*-1:*sn*-1'LPG (step 3), but the mechanism is still largely elusive. Next, *sn*-1:*sn*-1'LPG is acylated by a transacylase to yield *sn*-1:*sn*-1'BMP (step 4) (Amidon *et al.*, 1995).

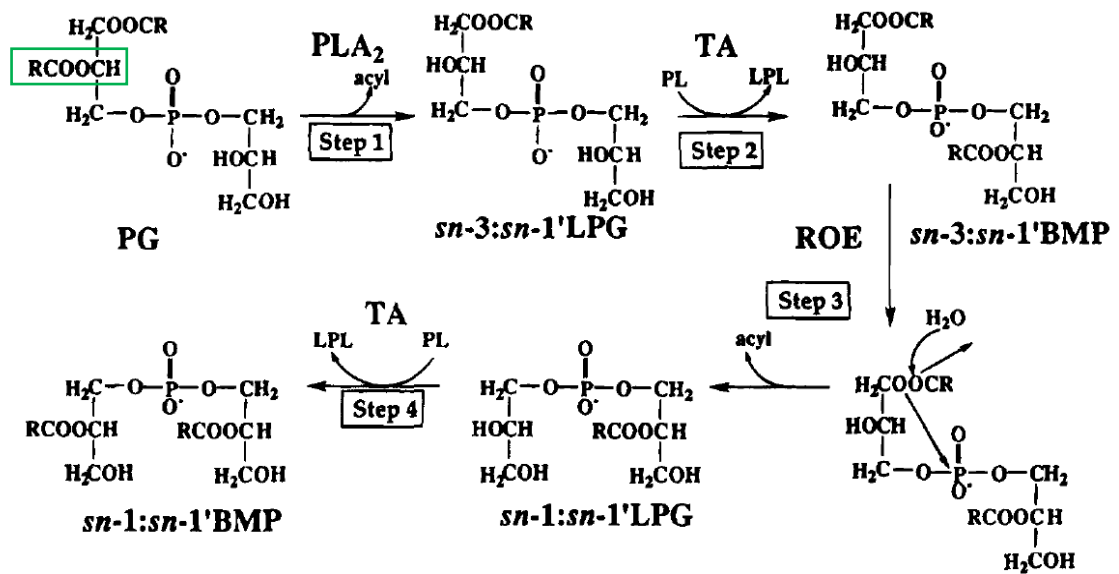


Figure 1.11: Proposed biosynthetic pathway of BMP from PG. PLA₂: Phospholipase A₂; TA: Transacylase; PL: Phospholipid; LPL: Lysophospholipid; ROE: Reorientation of enzyme (Amidon *et al.*, 1995)

Additionally, alternative routes for the biosynthesis of BMP have been proposed as depicted in figure 1.12. In hypothesis (1), deacylation/hydrolysis of PG leads to the formation of LPG, followed by the transfer of an acyl chain to the head group glycerol of LPG to form BMP, while the reorientation of the backbone occurs either during the first or second step. In hypothesis (2), an acyl chain is first transferred from an acyl donor to the head group glycerol of PG yielding an acyl phosphatidylglycerol (AcPG), followed by deacylation and concomitant reorientation to form BMP. The acylation process would be independent of acyl-CoA. Hypothesis (3) seems possible, though no experimental evidence to-date has been presented in its support (Poorthuis and Hostetler, 1976).